Front. Phys. 10, 100506 (2015)
DOI 10.1007/s11467-015-0473-1

RESEARCH ARTICLE

Rectification and phase locking of graphite

Zhen-Bin Zhang[1], Ru-Juan Jia[1], Jasmina Tekić[2], Yang Yang[1], Cang-Long Wang[3], Jia-Wei Li[4], Xiao-Yun Wang[5], Wen-Shan Duan[1,*], Lei Yang[3,†]

[1] *College of Physics and Electronic Engineering, Northwest Normal University, Lanzhou 730070, China*
[2] *Theoretical Physics Department 020, "Vinča" Institute of Nuclear Sciences, University of Belgrade, P.O. Box 522, 11001 Belgrade, Serbia*
[3] *Institute of Modern Physics, Chinese Academy of Sciences, Lanzhou 730000, China*
[4] *Department of Chemistry, Northwest Normal University, Lanzhou 730070, China*
[5] *Department of Mathematics and Physics, Lanzhou Jiao Tong University, Lanzhou 730070, China*
*Corresponding authors. E-mail: * duanws@nwnu.edu.cn, † lyang@impcas.ac.cn*
Received December 17, 2014; accepted May 3, 2015

Rectification phenomena and the phase locking in a two-dimensional overdamped Frenkel–Kontorova model with a graphite periodic substrate were studied. The presence of dc and ac forces in the longitudinal direction causes the appearance of dynamicalmode locking and the steps in the response function of the system. On the other hand, the presence of an ac force in the transverse direction causes the appearance of rectification,even though there is no net dc force in the transverse direction. It is found that whereas the longitudinal velocity increases in a series of steps, rectification in the transverse direction can occur only between two neighbor steps. The amplitude and phase of the external ac driving force affect the depinning force,rectification of the system and particles trajectories.

Keywords classical transport, friction and lubrication, computer simulation of molecular and particle dynamics

PACS numbers 05.60.Cd, 81.40.Pq, 83.10.Rs

Frontiers of Physics

1 Introduction

The properties of Shapiro steps [1, 2] have been studied experimentally and theoretically for many years in the dissipative dynamics of many-body systems, such as charge-density or spin-density wave conductors [3–7], vortex lattices [8–13], colloids [14, 15] and Josephson-junction arrays (JJA) biased by external currents [16–20]. To understand these very complex physical systems, the focus was always on simple many-body models. Among them, the dissipative (overdamped) Frenkel–Kontorova (FK) model [21–30] is one of the simplest and most tractable, yet it is still able to describe the essence of many physical and biological phenomena.

The FK model represents a harmonic chain of interacting particles subjected to a sinusoidal substrate potential [26, 31]. It can describe different commensurate or incommensurate structures that show very rich dynamical behavior when they are subjected to an external force. The dynamics of the dc+ac driven FK model is characterized by the appearance of a staircase macroscopic response or Shapiro steps in the curve of the average velocity as a function of the average external driving force. These phenomena are due to interference or dynamical locking of the internal frequency arising from the motion of particles over the periodic substrate potential with the frequency of an external ac force [32–34]. However, most works on the overdamped FK model consider only the simplest case in which the ac and dc forces are in the same direction. This raises the question of what type of phenomena will appear if the ac and dc forces are applied in different directions.

Attention has been focused recently on dissipative nonequilibrium systems which can produce a ratchet effect. For a particle moving in an asymmetric potential, a net dc drift in one direction can occur in the absence of a dc drive when an applied ac drive is combined with ac flashing of the potential. Rectification arises because of the asymmetric potential, which is the key factor for the appearance of this phenomenon in these one-dimensional (1D) systems. Such ratchet phenomena have been re-

© Higher Education Press and Springer-Verlag Berlin Heidelberg 2015

ported in a variety of 1D systems or motions, such as biological motors [35, 36], particle segregation [35–37], colloidal particles moving through asymmetric potentials [35, 36, 38], atom transport in optical lattices [39], charge transport in quantum dot systems [40], fluxon motion in superconductors [41, 42], transport of granular particles [43], and vortices in superconductors and superconducting quantum interference devices [44, 45].

There are many examples of rectification in two-dimensional (2D) systems, including the motion of biomolecules or polymers through periodic arrays of posts [46–48]. Here the particles are driven in alternating directions by an electric field. Another approach to 2D rectification is to drive particles through a periodic array at various angles [49–51]. Several theoretical studies have also considered models of particles moving in 2D asymmetric potentials, leading to rectification and negative differential conductivity [52–54]. A better understanding of 2D systems that exhibit rectification can facilitate the creation of technological devices for applications such as the separation of different species of colloids or biomolecules or new techniques for electrophoresis.

Graphene, a single, one-atom-thick sheet of carbon atoms arranged into a hexagonal honeycomb lattice, has excellent electronic, mechanical, and thermal properties and has exhibited great potential for a wide range of research in materials science and engineering. Graphene and its derivatives can be used as the active material in solar cells or transparent conductive electrodes, electrocatalysts for oxygen reduction in fuel cells, counter electrodes in dye-sensitized solar cells, and high-performance electrodes in supercapacitors, actuators, batteries, and sensors [55–57], and for electronic transport in quantum-dot structures [58–60].

Rectification of the simple cubic lattice and triangular lattice have been studied previously [21, 25]. The present study considers graphene, which is much more interesting. For example, the electrical and mechanical properties of graphene have been used in flexible transparent electrodes [61]. Stiff and flexible graphene oxide paper [62] is promising for use in fuel cells and structural composite applications. A nanoresonator based on flexural vibrations of suspended graphene was implemented [63]. Self-retracting motion of graphite was observed experimentally [64]. Nanorelays based on the telescopic motion of nanotube walls [65, 66] were realized experimentally. Furthermore, a mass nanosensor based on the small translational vibrations of nanotube walls was considered [67, 68]. By analogy with these devices, a nanorelay based on the telescopic motion of graphene layers and a mass nanosensor based on the small translational vibrations of graphene layers was proposed [69]. For all these applications and for understanding of the fundamental properties of graphene, the investigation of the mechanical properties of few-layer graphene associated with the relative displacement of the layers is highly important. The interaction between the walls of carbon nanotubes and between the nanotubes themselves is similar to the interaction between graphene layers. Therefore, investigation of the interlayer interaction and relative displacement of graphene layers is also of interest for the development of nanotube-based nanoelectromechanical systems [65–68, 70] and for studies of the interaction between carbon nanotubes in fibers and yarns [71].

In the theory of rectification phenomena, the dissipative 2D FK model driven by external dc and ac forces, where the ac force can be applied in both directions, has not been studied yet. In this paper, we investigate rectification and phase locking in the 2D overdamped FK model with a periodic graphite substrate where in addition to the dc and ac drives in the longitudinal direction, an ac force in the transverse direction is also applied. The rectification phenomena in the 2D FK model exhibit completely different physics from those in the 1D case [24, 72–75]. The longitudinal velocity was found to increase in a series of steps as F_{dc} increases where near the transition between two steps, rectification in the transverse direction was observed. The effect of the amplitude and phase of the external ac driving force on the rectification, critical depinning force and particle trajectories were investigated.

2 Model

In the overdamped FK model, the dynamics of the entire system is described by the following equation of motion:

$$\gamma\dot{\boldsymbol{r}}_{n,m} = -\frac{\partial(V_{int}+V_{sub})}{\partial \boldsymbol{r}_{n,m}} + \boldsymbol{F}(t), \tag{1}$$

where γ is the damping coefficient where in our work, simulations were performed for $\gamma = 1.0$, $\boldsymbol{r}_{n,m} = (x_{n,m}, y_{n,m})$ is the position of the (n,m)-th atom, V_{int} is the interatomic interaction potential, V_{sub} is the periodic substrate potential, and $\boldsymbol{F}(t) = \boldsymbol{F}_{dc} + \boldsymbol{F}_{ac}(t)$ is the driving force, where $\boldsymbol{F}_{dc} = F_{dc}\boldsymbol{x}$, $\boldsymbol{F}_{ac}(t) = A\sin(2\pi\nu_A t)\boldsymbol{x} + B\sin(2\pi\nu_B t + \phi_0)\boldsymbol{y}$, and $\boldsymbol{x}$ and $\boldsymbol{y}$ are the unit vectors in the longitudinal (x) and transverse (y) direction, respectively. We will consider a periodic pinning potential with hexagonal symmetry of graphite: $V_{sub} = V_0[2\cos(\frac{2\pi}{b}x)\cos(\frac{2\pi}{b\sqrt{3}}y) + \cos(\frac{4\pi}{b\sqrt{3}}y)]$, where b is the lattice constant of the substrate. The interaction potential between atoms in the upper layers of the graphitic layer is chosen to be of the simple harmonic

form $V_{int} = \sum_{n,m=1}^{20} \frac{K}{2}[(r_{n,m} - a)^2]$, with a stiffness strength K, where $r_{n,m}$ is the distance between two neighbors ($a = 0.246$ is the lattice constant of the upper layer).

In this paper, we consider the system size $14a \times \frac{9}{2}\sqrt{3}a$. The initial condition is that the velocities of all the atoms are zero, and all the atoms are in their equilibrium positions. Equation (1) is integrated using the fourth-order Runge–Kutta method with the periodic boundary conditions. The time step used in the simulations was 0.001τ, and a time interval of 100τ was used as a relaxation time to allow the system to reach the steady state. The dc force was increased from zero with the step 10^{-4}. We fix $\nu_A = \nu_B = \nu_0$, $A = B$ and examined the time average of both the longitudinal $\bar{v}_x$ and the transverse $\bar{v}_y$ velocities of particles. The response functions $\bar{v}_x(F_{dc})$ and $\bar{v}_y(F_{dc})$ were analyzed for the commensurate structure. In particular, the rectification, critical depinning force and particle trajectories are examined for different parameters of the system.

The response functions in the 1D FK model have been well studied, the average velocity of the resonant solution is given by $\bar{v} = \frac{i\beta+j}{m}\nu_0$ [32, 33, 74, 75], where i, j, and m are integers, and ν_0 is the frequency of the ac force. For a given resonant velocity value $\bar{v}$, the triplet (i, j, m) of integers is clearly not unique; if β is an irrational number, there is a unique minimal triplet with the property that i, j, and m have no common factors. On the other hand, for a rational value of $\beta = \frac{p}{q}$ (where p and q are co-prime integers), a minimal triplet is such that $ip + jq$ and m have no common factors. Accordingly, the resonant velocity is called harmonic if $m = 1$, and subharmonic whenever $m > 1$. When $\beta = 1$, $i = 0, m = 3$, the resonant solution is: $\bar{v}_x = \frac{j}{3}\nu_0$ $(j = 0, 1, 2, 3, \cdots)$, which is consistent with the results presented in Fig. 1.

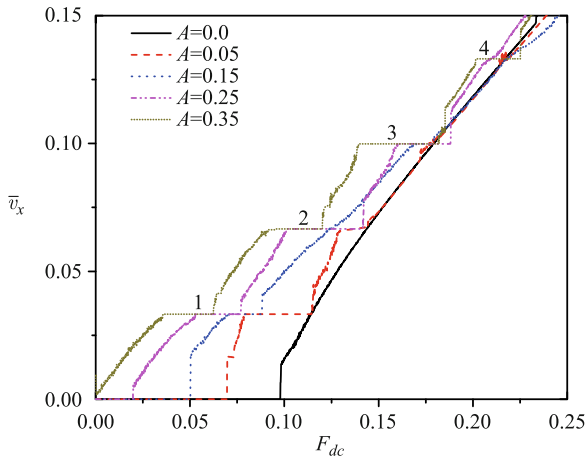

Fig. 1 Average velocity in the x-direction $\bar{v}_x$ as a function of the average driving force F_{dc} for $A = B$, $\phi_0 = 0$, $\nu_A = \nu_B = 0.1$ in different ac amplitude regime $A = 0, 0.05, 0.15, 0.25, 0.35$.

3 Numerical results

Figure 1 shows the response functions of $\bar{v}_x(F_{dc})$ are presented for the different amplitudes of the ac force. The response function is characterized by the appearance of large harmonic steps where the step width and the critical depinning force are strongly affected by the amplitude of the ac force. When $F_{ac} \to 0$, the system behaves as a dc-driven system. If an external ac force is applied, the average velocity of the resonant solution for the graphite system appears in a series of steps $\bar{v}_x = \frac{j}{3}\nu_0$ $(j = 0, 1, 2, 3, \cdots)$. On the jth step, the average velocity in the y direction is strictly zero. The quantization of the step height appears due to the periodicity of the external drive. This result differs from that obtained for the structure with the hexagonal symmetry in which $\bar{v}_x = j\nu_0$ [21]. The number of harmonic steps on the curves depends on the amplitude of the ac force. Namely, as we can see in Fig. 1, the first and the second steps appear for $A = 0.05$, the first and third steps appear for the case of $A = 0.15$, for the case of $A = 0.25$ there is no fourth step, and for the case $A = 0.35$, there are four steps. Very small subharmonic steps appear for the case $A = 0.05$ and $A = 0.35$.

Figure 2 shows $\bar{v}_x(F_{dc})$ and $\bar{v}_y(F_{dc})$ versus F_{dc} for $A = B = 0.25$, $\phi_0 = 0$ and $\nu_A = \nu_B = 0.1$. Because there is no net dc force in the transverse direction, $\bar{v}_y = 0$ for most values of F_{dc}. On the step of $\bar{v}_x(F_{dc})$, $\bar{v}_y(F_{dc})$ is zero, i.e., there is no rectification. However, the minimum value of the $\bar{v}_y$ appears in the negative direction, and the rectifications $(\bar{v}_y \neq 0)$ occur between two neighboring steps. As we can see in Fig. 2(b), the first rectification in the y-direction occurs between zero and the first step, and other rectifications in the positive y-direction occur

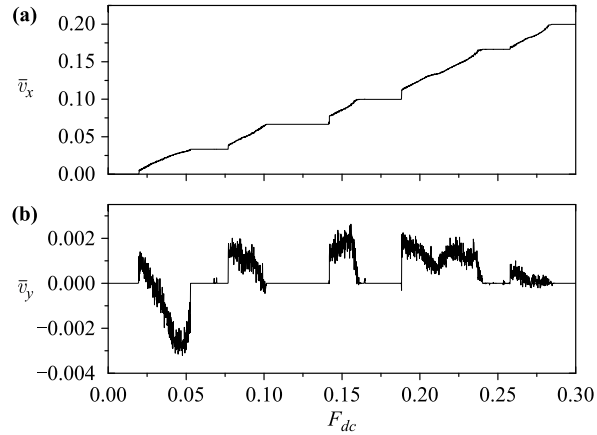

Fig. 2 **(a)** Longitudinal average velocity $\bar{v}_x$ vs. average driving force F_{dc} which is applied in the x-direction. **(b)** Corresponding average transverse velocity $\bar{v}_y$ vs. average driving force F_{dc} for $A = B = 0.25$, $\phi_0 = 0$, $\nu_A = \nu_B = 0.1$.

between two successive neighboring steps. The velocity in the x-direction is larger than that in the y-direction.

Figure 3 shows $\bar{v}_x(F_{dc})$ and $\bar{v}_y(F_{dc})$ as a function of F_{dc} for the ac amplitude $A = B = 0.2$ are presented (the other parameters are the same as in Fig. 2). A comparison of Fig. 3 and Fig. 2 reveals the strong effect of the ac amplitude on the results. In Fig. 2 the first rectification is mainly in the negative y-direction and the rectifications between steps all have similar values $\bar{v}_y(F_{dc})$. In Fig. 3, a very strong rectification with very large $\bar{v}_y(F_{dc})$ appears between the second and the fourth steps. Values of $A = B = 0.0, 0.05, 0.1, 0.15, 0.3, 0.35, 0.4, 0.5$, and 0.6 were also examined. Rectification can occur asymmetrically, it can appear in the positive or negative y-direction, depending on the magnitude of A.

The phase difference between the ac forces in the x- and y-directions strongly affects the rectification, as can

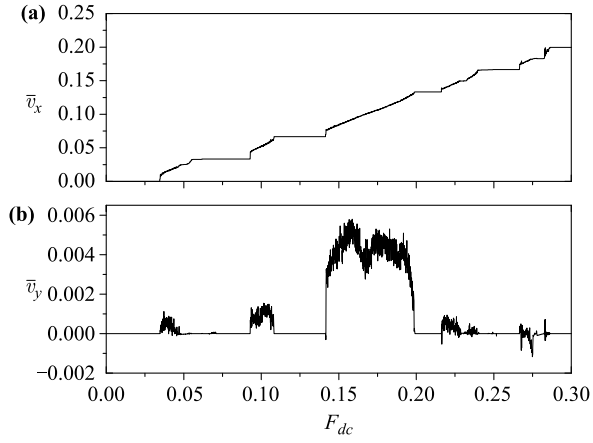

Fig. 3 **(a)** Longitudinal average velocity $\bar{v}_x$ vs. average driving force F_{dc} which is applied in the x-direction. **(b)** Corresponding average transverse velocity $\bar{v}_y$ vs. average driving force F_{dc} for $A = B = 0.2$, $\phi_0 = 0$, $\nu_A = \nu_B = 0.1$.

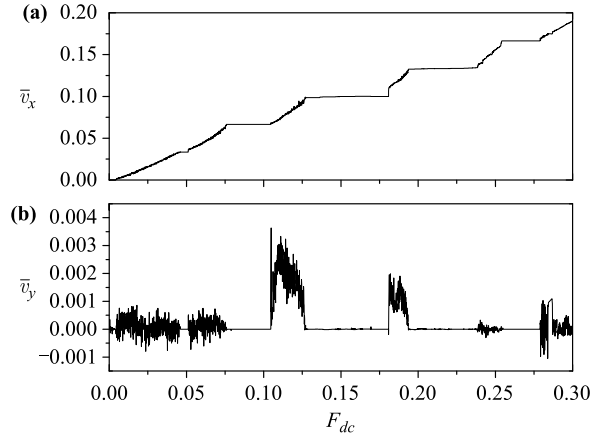

Fig. 4 **(a)** Longitudinal average velocity $\bar{v}_x$ vs. average driving force F_{dc} which is applied in the x-direction. **(b)** Corresponding average transverse velocity $\bar{v}_y$ vs. average driving force F_{dc} for $A = B = 0.2$, $\phi_0 = \frac{\pi}{2}$, $\nu_A = \nu_B = 0.1$.

beseen in Fig. 4, which shows the longitudinal and transverse velocities as a function of the average driving force are presented for $\phi_0 = \frac{\pi}{2}$ (the other parameters are the same as in Fig. 3. To understand how the phase difference affects the rectification in detail, the dependence of both $\bar{v}_x(F_{dc})$ and $\bar{v}_y(F_{dc})$ on F_{dc} for other values of $\phi_0 = 0, \frac{\pi}{6}, \frac{\pi}{4}, \frac{\pi}{3}, \frac{\pi}{2}$ were examined. Figure 5 shows the results obtained for the case of $\phi_0 = \frac{\pi}{4}$. These results also show the effect of the phase on the critical depinning force. For $A = B = 0.2$ in Fig. 3, the critical depinning force is nonzero, whereas with the introduction of the phase difference in Figs. 4 and 5, the critical depinning force at which rectification is observed decreases to zero as ϕ_0 increases.

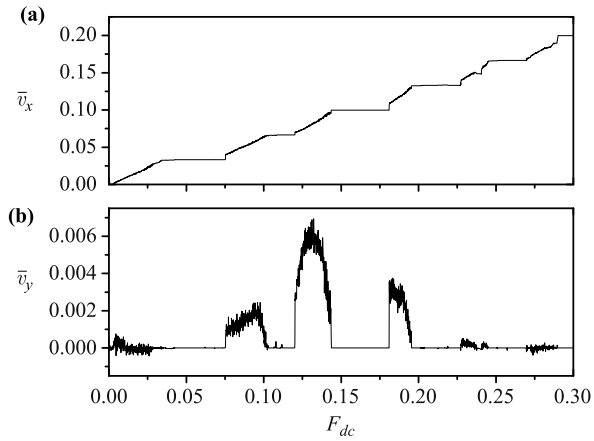

Fig. 5 **(a)** Longitudinal average velocity $\bar{v}_x$ vs. average driving force F_{dc} which is applied in the x-direction. **(b)** Corresponding average transverse velocity $\bar{v}_y$ vs. average driving force F_{dc} for $A = B = 0.2$, $\phi_0 = \frac{\pi}{4}$, $\nu_A = \nu_B = 0.1$.

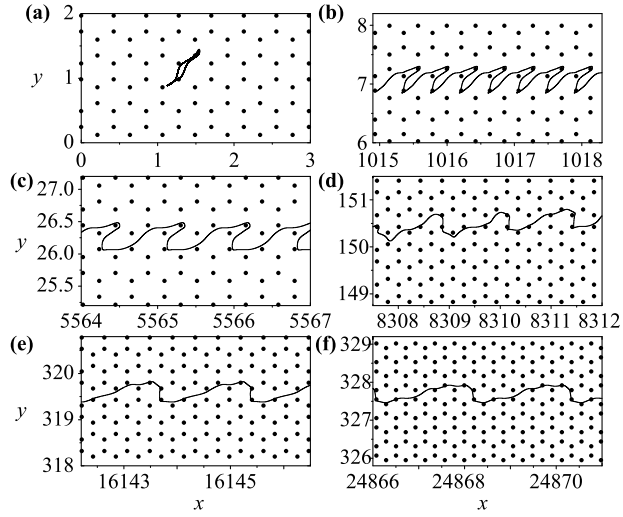

Fig. 6 Particle trajectories (*black lines*) and periodic potential minima (*black dots*) for different dc forces F_{dc} from Fig. 3. **(a)** $F_{dc} = 0$, **(b)** $F_{dc} = 0.0711$, **(c)** $F_{dc} = 0.1388$, **(d)** $F_{dc} = 0.1641$, **(e)** $F_{dc} = 0.2153$, **(f)** $F_{dc} = 0.2590$.

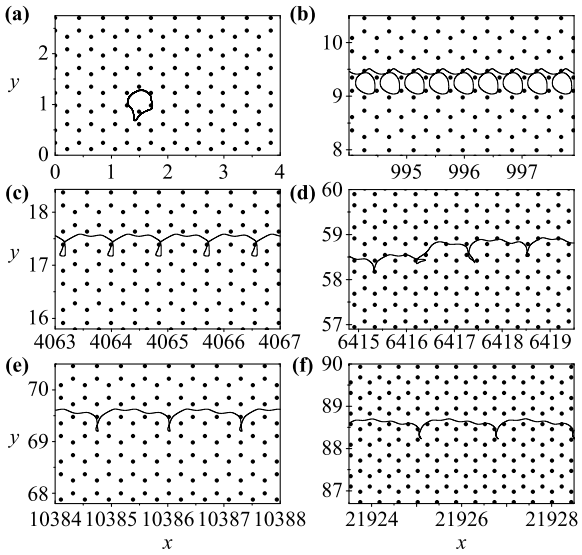

Fig. 7 Particle trajectories (*black lines*) and periodic potential minima (*black dots*) for different dc forces F_{dc} from Fig. 4. **(a)** $F_{dc} = 0$, **(b)** $F_{dc} = 0.05$, **(c)** $F_{dc} = 0.0943$, **(d)** $F_{dc} = 0.1198$, **(e)** $F_{dc} = 0.1519$, **(f)** $F_{dc} = 0.2281$.

To understand how the steps and the rectification appear, the particle trajectories were analyzed. The trajectories of one particle moving on the substrate potential are presented for six different cases of $\bar{v}_x$: the zero step ($j = 0$), the first harmonic ($j = 1$), the second one ($j = 2$), the transition from the second to the third one ($j = 2 \to 3$), the third ($j = 3$) and the fourth step ($j = 4$) in Figs. 6(a)–(f) respectively, where $A = B = 0.2$, $\nu_A = \nu_B = 0.1$ and $\phi_0 = 0$.

In Fig. 6(a), $F_{dc} = 0$ ($j = 0$), where $\bar{v}_x(F_{dc}) = \bar{v}_y(F_{dc}) = 0$, the particle moves in a confined orbit that encircles one pin. When the particle is on the first step (the average velocity is a constant in the x direction) in Fig. 6(b), $F_{dc} = 0.0711$ ($j = 1$), and the orbit does not encircle a pin but forms a small loop that repeats every first plaquette. Because the average velocity is zero in the y direction, there is no rectification in this case. The results in Figs. 6(c) ($j = 2$), (e) ($j = 4$), and (f) ($j = 5$) are similar to that in Fig. 6(b). The average velocity in the y direction is zero for these cases, suggesting that no rectification occurs. In one period, the displacement in the x direction is $2b$, $4b$ and $5b$ respectively. However, in the transitional region between steps 2 and 3 ($j = 2 \to 3$) in Fig. 6(d), the rectification occurs. The displacement of the particle in the x direction is $3b$, whereas that in the y direction is nonzero.

Changing of the phase ϕ_0 will affect these trajectories. Figure 7 shows the one particle trajectory for the case of $A = B = 0.2$, $\nu_A = \nu_B = 0.1$ and $\phi_0 = \frac{\pi}{2}$. The dc forces are $F_{dc} = 0, 0.05, 0.0943, 0.1198, 0.1519$, and 0.2281 in Fig. 7(a)–(f) respectively. As in the previous case in Fig. 6, in Fig. 7(d), rectification appears between two steps, $j = 2 \to 3$, where $F_{dc} = 0.1198$.

Similar results were also observed for the other system parameters. On the basis of these simulations, we find that the rectifications always occurs between two neighboring steps. On the steps, there are no rectification phenomena.

4 Conclusion

In conclusion, the dynamics of a 2D overdamped Frenkel–Kontorova model with a periodic graphite substrate in the presence of dc and ac forces was studied, where the ac force is applied in both the longitudinal and transverse directions. The obtained results showed that whereas the longitudinal velocity increases in a series of steps of the height $\frac{j}{3}\nu_0$, the rectification ($\bar{v}_y \neq 0$) may occur in the transition region between two neighboring steps of $\bar{v}_x$. By changing the amplitudes and the phase of the external ac force, one can control the rectification, trajectories and depinning of particles, i.e., the frictional force in the system. These results may have potential applications in many branches of physics such as studies of vortices in superconductors, classical electron motion, and biomolecules moving through 2D arrays of posts, and especially in nanotribology.

This study differs from the previous works [21, 25]. The rectification of materials with triangular symmetry was studied in Ref. [21], whereas that of the simple cubic symmetric materials was studied in Ref. [25]. The present study,unlike all other previous works, considers graphite.

Acknowledgements This work was supported by the "Strategic Priority Research Program" of the Chinese Academy of Sciences (Grant No. XDA03030100), and the National Natural Science Foundation of China (Grant Nos. 11275156 and 11304324). This work was partly supported by the Serbian Ministry of Education and Science under Contracts No. III-45010.

References

1. S. Shapiro, Josephson currents in superconducting tunneling: The effect of microwaves and other observations, *Phys. Rev. Lett.* 11(2), 80 (1963)
2. C. C. Grimes and S. Shapiro, Millimeter-wave mixing with Josephson junctions, *Phys. Rev.* 169(2), 397 (1968)
3. G. Grüner, The dynamics of charge-density waves, *Rev. Mod. Phys.* 60(4), 1129 (1988)
4. R. E. Thorne, J. S. Hubacek, W. G. Lyons, J. W. Lyding, and J. R. Tucker, ac-dc interference, complete mode locking, and origin of coherent oscillations in sliding charge-density-wave systems, *Phys. Rev. B* 37(17), 10055 (1988)

5. G. Kriza, G. Quirion, O. Traetteberg, W. Kang, and D. Jérome, Shapiro interference in a spin-density-wave system, *Phys. Rev. Lett.* 66(14), 1922 (1991)
6. J. McCarten, D. A. DiCarlo, M. P. Maher, T. L. Adelman, and R. E. Thorne, Charge-density-wave pinning and finite-size effects in $NbSe_3$, *Phys. Rev. B* 46(8), 4456 (1992)
7. S. N. Coppersmith and P. B. Littlewood, Interference phenomena and mode locking in the model of deformable sliding charge-density waves, *Phys. Rev. Lett.* 57(15), 1927 (1986)
8. C. Reichhardt, C. J. O. Reichhardt, and M. B. Hastings, Nonlinear dynamics, rectification, and phase locking for particles on symmetrical two-dimensional periodic substrates with dc and circular ac drives, *Phys. Rev. B* 69(5), 056115 (2004)
9. J. Y. Lin, M. Gurvitch, S. K. Tolpygo, A. Bourdillon, S. Y. Hou, and J. M. Phillips, Flux pinning in $YaBa_2Cu_3O_{7-\delta}$ thin films with ordered arrays of columnar defects, *Phys. Rev. B* 54(18), R12717 (1996)
10. T. Giamarchi and P. Le Doussal, Moving glass phase of driven lattices, *Phys. Rev. Lett.* 76(18), 3408 (1996)
11. D. Perez de Lara, L. Dinis, E. M. Gonzalez, J. M. R. Parrondo, J. V. Anguita, and J. L. Vicent, Rocking ratchets in nanostructured superconducting–magnetic hybrids, *J. Phys.: Condens. Matter* 21(25), 254204 (2009)
12. J. C. Ciria and C. Giovannella, Vortex dynamics in classical Josephson junction arrays: Models and recent experimental developments, *J. Phys.: Condens. Matter* 10(7), 1453 (1998)
13. C. Reichhardt and C. J. Olson Reichhardt, Structural transitions and dynamical regimes for directional locking of vortices and colloids driven over periodic substrates, *J. Phys.: Condens. Matter* 24(22), 225702 (2012)
14. C. Reichhardt and C. J. O. Reichhardt, Local melting and drag for a particle driven through a colloidal crystal, *Phys. Rev. Lett.* 92(10), 108301 (2004)
15. M. Mikulis, C. J. Olson Reichhardt, C. Reichhard, R. T. Scalettar, and G. T. Zimányi, Reentrant disordering of colloidal molecular crystals on 2D periodic substrates, *J. Phys.: Condens. Matter* 16, 7909 (2004)
16. B. D. Josephson, Supercurrents through barriers, *Adv. Phys.* 14(56), 419 (1965)
17. S. P. Benz, M. S. Rzchowski, M. Tinkham, and C. J. Lobb, Fractional giant Shapiro steps and spatially correlated phase motion in 2D Josephson arrays, *Phys. Rev. Lett.* 64(6), 693 (1990)
18. H. B. Wang, S. M. Kim, S. Urayama, M. Nagao, T. Hatano, S. Arisawa, T. Yamashita, and P. H. Wu, Shapiro steps observed in annular intrinsic Josephson junctions at low microwave frequencies, *Appl. Phys. Lett.* 88(6), 063503 (2006)
19. P. Komissinskiy, G. A. Ovsyannikov, K. Y. Constantinian, Y. V. Kislinski, I. V. Borisenko, I. I. Soloviev, V. K. Kornev, E. Goldobin, and D. Winkler, High-frequency dynamics of hybrid oxide Josephson heterostructures, *Phys. Rev. B* 78(2), 024501 (2008)
20. R. de Luca, Ratchet potential in superconducting quantum interference devices containing a double-barrier junction, *Supercond. Sci. Technol.* 22(8), 085008 (2009)
21. Y. Yang, W. S. Duan, L. Yang, J. M. Chen, and M. M. Lin, Rectification and phase locking in overdamped two-dimensional Frenkel–Kontorova model, *Europhys. Lett.* 93(1), 16001 (2011)
22. B. Hu and L. Yang, Heat conduction in the Frenkel–Kontorova model, *Chaos* 15(1), 015119 (2005)
23. B. Hu, L. Yang, and Y. Zhang, Asymmetric heat conduction in nonlinear lattices, *Phys. Rev. Lett.* 97(12), 124302 (2006)
24. C. L. Wang, J. Tekić, W. S. Duan, Z. G. Shao, and L. Yang, Existence and stability of the resonant phenomena in the dc- and ac-driven overdamped Frenkel–Kontorova model with the incommensurate structure, *Phys. Rev. E* 84(4), 046603 (2011)
25. C. L. Wang, J. Tekić, W. S. Duan, Z. G. Shao, and L. Yang, Ratchet effect and amplitude dependence of phase locking in a two-dimensional Frenkel–Kontorova model, *J. Chem. Phys.* 138(3), 034307 (2013)
26. O. M. Braun and Y. S. Kivshar, The Frenkel–Kontorova Model, Berlin: Springer, 2003
27. J. Tekić, O. M. Braun, and B. Hu, Dynamic phases in the two-dimensional underdamped driven Frenkel–Kontorova model, *Phys. Rev. E* 71(2), 026104 (2005)
28. J. A. van den Ende, A. S. de Wijn, and A. Fasolino, The effect of temperature and velocity on superlubricity, *J. Phys.: Condens. Matter* 24(44), 445009 (2012)
29. C. F. Kreiner and J. Zimmer, Existence of subsonic heteroclinic waves for the Frenkel–Kontorova model with piecewise quadratic on-site potential, *Nonlinearity* 24(4), 1137 (2011)
30. B. Hu, B. Li, and H. Zhao, Mode-locking of incommensurate phase by quantum zero-point energy in the Frenkel–Kontorova model, *Europhys. Lett.* 53(3), 342 (2001)
31. O. M. Braun and Y. S. Kivshar, Nonlinear dynamics of the Frenkel–Kontorova model, *Phys. Rep.* 306(1–2), 1 (1998)
32. L. M. Floría and J. J. Mazo, Dissipative dynamics of the Frenkel–Kontorova model, *Adv. Phys.* 45(6), 505 (1996)
33. F. Falo, L. M. Floría, P. J. Martínez, and J. J. Mazo, Unlocking mechanism in the ac dynamics of the Frenkel–Kontorova model, *Phys. Rev. B* 48(10), 7434 (1993)
34. M. Inui and S. Doniach, Use of few-domain classical models to study mode locking in charge-density-wave systems, *Phys. Rev. B* 35(12), 6244 (1987)
35. M. O. Magnasco, Forced thermal ratchets, *Phys. Rev. Lett.* 71(10), 1477 (1993)
36. R. D. Astumian, Thermodynamics and Kinetics of a Brownian Motor, *Science* 276(5314), 917 (1997)
37. J. L. Mateos, Chaotic transport and current reversal in deterministic ratchets, *Phys. Rev. Lett.* 84(2), 258 (2000)
38. R. Bartussek, P. Hänggi, and J. C. Kissner, Periodically rocked thermal ratchets, *Europhys. Lett.* 28(7), 459 (1994)

39. C. Mennerat-Robilliard, D. Lucas, S. Guibal, J. Tabosa, C. Jurczak, J. Y. Courtois, and G. Grynberg, Ratchet for cold rubidium atoms: The asymmetric optical lattice, *Phys. Rev. Lett.* 82(4), 851 (1999)
40. H. Linke, T. E. Humphrey, A. Lofgren, A. O. Sushkov, R. Newbury, R. P. Taylor, and P. Omling, Experimental tunneling ratchets, *Science* 286(5448), 2314 (1999)
41. A. V. Silhanek, W. Gillijns, V. V. Moshchalkov, V. Metlushko, F. Gozzini, B. Ilic, W. C. Uhlig, and J. Unguris, Manipulation of the vortex motion in nanostructured ferromagnetic/superconductor hybrids, *Appl. Phys. Lett.* 90(18), 182501 (2007)
42. C. C. de Souza Silva, J. Van de Vondel, M. Morelle, and V. V. Moshchalkov, Controlled multiple reversals of a ratchet effect, *Nature* 440(7084), 651 (2006)
43. Z. Farkas, P. Tegzes, A. Vukics, and T. Vicsek, Transitions in the horizontal transport of vertically vibrated granular layers, *Phys. Rev. E* 60(6), 7022 (1999)
44. J. F. Wambaugh, C. Reichhardt, C. J. Olson, F. Marchesoni, and F. Nori, Superconducting fluxon pumps and lenses, *Phys. Rev. Lett.* 83(24), 5106 (1999)
45. I. Zapata, R. Bartussek, F. Sols, and P. Hänggi, Voltage rectification by a SQUID ratchet, *Phys. Rev. Lett.* 77(11), 2292 (1996)
46. W. D. Volkmuth and R. H. Austin, DNA electrophoresis in microlithographic arrays, *Nature* 358(6387), 600 (1992)
47. T. A. J. Duke, and R. H. Austin, Microfabricated sieve for the continuous sorting of macromolecules, *Phys. Rev. Lett.* 80(7), 1552 (1998)
48. J. L. Viovy, Electrophoresis of DNA and other polyelectrolytes: Physical mechanisms, *Rev. Mod. Phys.* 72(3), 813 (2000)
49. C. Reichhardt and F. Nori, Phase locking, Devil's staircases, Farey trees, and Arnold tongues in driven vortex lattices with periodic pinning, *Phys. Rev. Lett.* 82(2), 414 (1999)
50. P. T. Korda, M. B. Taylor, and D. G. Grier, Kinetically locked-in colloidal transport in an array of optical tweezers, *Phys. Rev. Lett.* 89(12), 128301 (2002)
51. D. G. Grier, A revolution in optical manipulation, *Nature* 424(6950), 810 (2003)
52. G. A. Cecchi and M. O. Magnasco, Negative resistance and rectification in Brownian transport, *Phys. Rev. Lett.* 76(11), 1968 (1996)
53. R. Eichhorn, P. Reimann, and P. Hänggi, Brownian motion exhibiting absolute negative mobility, *Phys. Rev. Lett.* 88(19), 190601 (2002)
54. Z. Zheng, M. C. Cross, and G. Hu, Collective directed transport of symmetrically coupled lattices in symmetric periodic potentials, *Phys. Rev. Lett.* 89(15), 154102 (2002)
55. S. Stankovich, D. A. Dikin, G. H. B. Dommett, K. M. Kohlhaas, E. J. Zimney, E. A. Stach, R. D. Piner, S. B. T. Nguyen, and R. S. Ruoff, Graphene-based composite materials, *Nature* 442(7100), 282 (2006)
56. X. Li, G. Zhang, X. Bai, X. Sun, X. Wang, E. Wang, and H. Dai, Highly conducting graphene sheets and Langmuir–Blodgett films, *Nat. Nanotechnol.* 3(9), 538 (2008)
57. D. Yu and L. Dai, *Appl. Phys. Lett.* 96, 14310 (2010)
58. L. Huang, Y. C. Lai, D. K. Ferry, R. Akis, and S. M. Goodnick, Transmission and scarring in graphene quantum dots, *J. Phys.: Condens. Matter* 21(34), 344203 (2009)
59. L. Ying, L. Huang, Y. C. Lai, and Y. Zhang, Effect of geometrical rotation on conductance fluctuations in graphene quantum dots, *J. Phys.: Condens. Matter* 25(10), 105802 (2013)
60. L. Ying, L. Huang, Y. C. Lai, and C. Grebogi, Conductance fluctuations in graphene systems: The relevance of classical dynamics, *Phys. Rev. B* 85(24), 245448 (2012)
61. S. Bae, H. Kim, Y. Lee, X. Xu, J. S. Park, Y. Zheng, J. Balakrishnan, T. Lei, H. Ri Kim, Y. I. Song, Y.J. Kim, K. S. Kim, B. Özyilmaz, J. H. Ahn, B. H. Hong, and S. Iijima, Roll-to-roll production of 30-inch graphene films for transparent electrodes, *Nat. Nanotechnol.* 5(8), 574 (2010)
62. D. A. Dikin, S. Stankovich, E. J. Zimney, R. D. Piner, G. H. B. Dommett, G. Evmenenko, S. B. T. Nguyen, and R. S. Ruoff, Preparation and characterization of graphene oxide paper, *Nature* 448(7152), 457 (2007)
63. J. S. Bunch, A. M. van der Zande, S. S. Verbridge, I. W. Frank, D. M. Tanenbaum, J. M. Parpia, H. G. Craighead, and P. L. McEuen, Electromechanical resonators from graphene sheets, *Science* 315(5811), 490 (2007)
64. Q. Zheng, B. Jiang, S. Liu, Yu. Weng, L. Lu, Q. Xue, J. Zhu, Q. Jiang, S. Wang, and L. Peng, Self-retracting motion of graphite microflakes, *Phys. Rev. Lett.* 100(6), 067205 (2008)
65. V. V. Deshpande, H. Y. Chiu, H. W. Ch. Postma, C. Miko, L. Forro, and M. Bockrath, Carbon nanotube linear bearing nanoswitches, *Nano Lett.* 6(6), 1092 (2006)
66. A. Subramanian, L. X. Dong, B. J. Nelson, and A. Ferreira, Supermolecular switches based on multiwalled carbon nanotubes, *Appl. Phys. Lett.* 96(7), 073116 (2010)
67. E. Bichoutskaia, A. M. Popov, Yu. E. Lozovik, O. V. Ershova, I. V. Lebedeva, and A. A. Knizhnik, Modeling of an ultrahigh-frequency resonator based on the relative vibrations of carbon nanotubes, *Phys. Rev. B* 80(16), 165427 (2009)
68. E. Bichoutskaia, A. M. Popov, Yu. E. Lozovik, O. V. Ershova, I. V. Lebedeva, and A. A. Knizhnik, Nanoresonator based on relative vibrations of the walls of carbon nanotubes, *Fullerenes, Nanotubes, and Carbon Nanostructures* 18(4–6), 523 (2010)
69. I. V. Lebedeva, A. A. Knizhnik, A. M. Popov, Yu. E. Lozovik, and B. V. Potapkin, Interlayer interaction and relative vibrations of bilayer graphene, *Phys. Chem. Chem. Phys.* 13(13), 5687 (2011)
70. Yu. E. Lozovik and A. M. Popov, Properties and nanotechnological applications of nanotubes, *Physics-Uspekhi* 50(7), 749 (2007)

71. J. J. Vilatela, J. A. Elliott, and A. H. Windle, A model for the strength of yarn-like carbon nanotube fibers, *ACS Nano* 5(3), 1921 (2011)

72. C. Reichhardt, C. J. Olson, and M. B. Hastings, Rectification and phase locking for particles on symmetric two-dimensional periodic substrates, *Phys. Rev. Lett.* 89(2), 024101 (2002)

73. B. Hu and J. Tekić, Frequency oscillations of the Shapiro steps, *Appl. Phys. Lett.* 90(10), 102119 (2007)

74. B. Hu and J. Tekić, Amplitude and frequency dependence of the Shapiro steps in the dc- and ac-driven overdamped Frenkel–Kontorova model, *Phys. Rev. E* 75(5), 056608 (2007)

75. J. Tekić, and B. Hu, Properties of the Shapiro steps in the ac driven Frenkel–Kontorova model with deformable substrate potential, *Phys. Rev. E* 81(3), 036604 (2010)